

Strategies for model updating and structural health monitoring of wind turbine blades

Inês Fernandes
inesorfernandes@tecnico.ulisboa.pt

Instituto Superior Técnico, Universidade de Lisboa, Portugal

November 2022

Abstract

One of the most appealing renewable energy power sources is the wind. The greatest challenge of this growing sector is monitoring the condition of the wind turbine structures. They are vulnerable to damage and deterioration, because they operate under large mechanical and aerodynamic loads and extreme environmental conditions. Developing Structural Health Monitoring (SHM) strategies is crucial to ensure that damages are detected effectively. In this thesis, three Machine Learning (ML) damage detection methodologies are tested: Multivariate Gaussian Anomaly Detection (MGAD), Principal Component Analysis (PCA) and Anomaly Detection Autoencoder (ADAE). These techniques were implemented to recognize deviating patterns from the healthy state to the damaged state of a structure. The data was acquired experimentally from a Glass-Fiber Reinforced Polymer (GFRP) scaled blade and features were extracted, such as modal parameters, Frequency Response Functions (FRFs) and acceleration time signals. In response to the data scarcity barrier imposed by the experimental data on the potential of ML algorithms, the second part of this thesis turns to the Finite Element Method (FEM). For the use of simulation data to be successfully applied to real situations, it needs to be a reliable representation of reality. One way of accomplishing this is by developing model updating strategies. Making use of a Finite Element (FE) model of the blade studied before, its parameters are tuned in order to reduce the differences in the experimental response data and the predicted by the FE model

Keywords: wind turbine blade, Structural Health Monitoring, damage detection, Machine Learning, Frequency Response Function, model updating.

1. Introduction

Wind is one of the most appealing renewable energy power sources, and it is becoming a more and more relevant source of energy production [1]. It happens often that the best locations for generating wind power are remote, where Wind Turbine (WT) structures are exposed to extreme settings. Therefore it is common that they sustain operational damage, thus the maintenance of these is crucial [2]. In order to optimize these procedures, the development of Structural Health Monitoring strategies help detect damage effectively.

Machine Learning (ML) algorithms are a good way to automate damage detection procedures while also improving accuracy [3]. In this thesis, using dynamic analysis concepts certain data (modal parameters, Frequency Response Functions, acceleration time signals) were extracted from experimental vibration measurements. Which served as features when testing different ML methodologies for damage detection.

A common issue in most Artificial Intelligence approaches is the need for significant amounts of varied training data. Experimental data from physical structures is not only impractical to collect it is also limited in scenarios. This is where FEM comes in with the possibility of generating a limitless number of training examples, with any type of configuration and properties, capturing a wide range of operating conditions.

In order to obtain a high-fidelity finite element model its parameters can be tuned through model updating strategies, with the objective of generating simulation vibration response data as similar as possible to the measured data [4]. A model updating strategy is proposed in this study, correlating the simulation model responses with the experimentally measured ones. In search for making them as similar as possible, some parameters of the finite element model are tuned.

2. Theoretical Background

2.1. Numerical Dynamic Analysis

In dynamic analysis, opposed to static analysis, dynamic loads are applied as a function of time, causing a time-varying response (displacements, velocities, accelerations, forces and stresses). In this study, dynamic analysis was performed on the data gathered from dynamic and structural simulations using the Siemens Simcenter™ 3D software, complemented with the Simcenter™ NASTRAN® as FEM solver [5].

2.1.1 Normal Modes Analysis

Generally, the first stage in dynamic analysis is the normal modes analysis (SOL 103), which is a process of studying a structure and estimating its modal parameters such as natural frequencies, damping ratios and mode shapes. The equation of motion of a Multi-

ple Degree-of-Freedom (MDOF) system is given by the following equilibrium equation:

$$[M]\{\ddot{x}\} + [C]\{\dot{x}\} + [K]\{x\} = \{F\} \quad (1)$$

Where $[M]$ is the matrix of the total mass, $[C]$ the matrix of the total damping and $[K]$ the matrix of the total stiffness. Each displacement is represented by the response vector $x(t)$ and the excitation given to the system is described by the forcing vector $F(t)$. One can determine the natural frequencies and the mode shapes of a structure, by analysing the oscillatory system's behavior when no external forces are applied. Analytically, this translates to solving the reduced form of the equation of motion where the force vector is null, turning this into an eigenvalue problem. To solve Equation 1, a harmonic solution of the following form is assumed:

$$\{x(t)\} = \{u\} \cos(\omega t - \phi) \quad (2)$$

Where u is the modal vector, which describes the spatial configuration of the system's DOF at a particular circular natural frequency ω and with a particular phase shift ϕ . When the assumed harmonic solution is differentiated and substituted into the motion equation, for $\cos(\omega t - \phi) \neq 0$, the following is obtained:

$$[[K] - \omega^2[M]] \{u\} = 0$$

This equation is called the eigenproblem, which has the eigenvalues (frequencies) and eigenvectors (vibration modes) as solutions. The non-trivial solution of this equation, $\det [[K] - \omega^2[M]] = 0$, has a discrete set of n solutions corresponding to the n normal vibration modes. Each mode has its particular natural frequency ω_i and mode shape u_i .

2.1.2 Modal Frequency Response Analysis

Frequency response analysis is used to compute the structural response to steady-state oscillatory stimulation, where the excitation is explicitly defined in the frequency domain. The modal frequency response analysis (SOL 111), resorting to the aforementioned eigenvalue analysis, utilizes the mode shapes of the structure. The solution at a specific frequency is the result of the summation of the individual modal responses.

In a modal solver the equation of motion (Equation 1) is solved with the same harmonic solution as before (Equation 2), but first the response is transformed from physical coordinates, $\{u(\omega)\}$, to modal coordinates, $\{\eta(\omega)\}$ making use of mode shapes, $[\Phi]$:

$$\{x(t)\} = [\Phi]\{\eta(\omega)\}e^{j\omega t}$$

The i^{th} equation of motion can be written as a set of single DOF systems in the uncoupled form:

$$-\omega^2 m_i \eta_i(\omega) + k_i \eta_i(\omega) = f_i(\omega)$$

Where m_i is the modal mass, k_i the modal stiffness and f_i the modal force of the i^{th} mode.

2.1.3 Modal Transient Response Analysis

Transient response analysis is the most common approach when calculating forced dynamic response. The goal is computing the behavior of a structure that has been exposed to time-varying excitation. The transient excitation is explicitly defined in the time domain, being that at each point in time, the structure's total applied loads are known. The modal transient response method solves the equation of motion in the modal domain, therefore reducing largely the number of unknowns and computational effort, since the modal domain is then used to compute the solution for the time domain. Rewriting the equations of motion (Equation 1) in the modal basis, so that they represent a collection of systems with a single DOF, in the time domain:

$$m_i \ddot{\eta}_i(t) + k_i \eta_i(t) = f_i(t)$$

2.2. Experimental Modal Analysis

In order to use Experimental Modal Analysis (EMA), it is required that both the input and the output forces be known. With this data it is possible to calculate the frequency domain ratio between the output and the input, resulting in the FRFs. In Equation 3, $[H(j\omega)]$ is a matrix containing all the FRFs. So these functions describe how the structure moves at each measurement location per unit force at the input location [6]. The basis of EMA is that FRFs can be written in terms of modal parameters, therefore they can be extracted [7].

$$X(j\omega) = [H(j\omega)]F(j\omega) \quad (3)$$

A modal parameter estimator computes the so called stabilization diagram, which is a combined representation of the measurement data and the system poles containing the modal parameter information [8]. In the framework of this thesis, the acquired FRFs were processed using Siemens SimcenterTM TestlabTM software. The analysis of a stabilization diagram involves the interactive selection of poles, these are calculated by modal parameter estimation methods. The one used for this study was the Polymax algorithm, also known as the polyreference least squares complex frequency domain method (p-LSCFD) [9]. After the pole selection, the algorithm estimates the modal parameters [10].

2.3. Machine Learning

The ML algorithms used in this work were the Multivariate Gaussian Anomaly Detection (MGAD), Principal Component Analysis (PCA) and Anomaly Detection Autoencoder (ADAE).

2.3.1 Multivariate Gaussian Anomaly Detection

This algorithm fits a Multivariate Gaussian distribution to a healthy subset of features (Equation 4).

$$p(x, \mu, \Sigma) = \frac{1}{(2\pi)^{n/2} |\Sigma|^{1/2}} \exp\left(-\frac{1}{2}(x - \mu)^T \Sigma^{-1} (x - \mu)\right) \quad (4)$$

Where $\mu \in \mathbb{R}^M$ is the mean vector of the feature's distribution and is defined as:

$$\mu = \frac{1}{N} \sum_{i=1}^N x^{(i)} \quad (5)$$

And the covariance matrix ($\Sigma \in \mathbb{R}^{M \times M}$) as:

$$\Sigma = \frac{1}{N} \sum_{i=1}^N (x^{(i)} - \mu) (x^{(i)} - \mu)^T \quad (6)$$

Then, an optimal threshold is calculated by a threshold selection process to differentiate examples corresponding to anomalies from ones expressing acceptable values. The premise is that data from the damaged structure will be outliers.

2.3.2 Principal Component Analysis

Principal Components (PCs) are a set of orthogonal variables that are computed via PCA from the input data and are able to statistically describe this data. PCs may project the original data into a lower dimensions orthogonal subspace, reducing highly dimensional data to its essential components.

The PCA computation is based on Singular Value Decomposition (SVD). The SVD of a data matrix $X \in \mathbb{R}^{N, M}$, with N data examples and M normalized features, is denoted as follows:

$$[U, S, V^T] = svd(X)$$

Where U represents the left singular vectors, with each row-vector representing a particular data example and the newly calculated features, which are still not scaled by the singular values; S contains the singular values organized by importance; and V^T represents the right singular vectors where each row-vector represents the PCs or directions to project the data. By lowering V^T , as defined in Equation 7, it is possible to choose a smaller set of k PCs from the data.

$$V_{reduced}^T = V^T(1 : k, :) \quad (7)$$

In this work, a subspace representation of the PCs from a healthy structure is stored in a $V^T \in \mathbb{R}^{k, M}$, which is later used to create a damage detection tool. A new data matrix $Y \in \mathbb{R}^{N_2, M}$ containing N_2 new measurements and M features can be projected into the previous PCs as follows:

$$Y_{reduced} = Y \times V_{reduced}$$

In Equation 8, Y is transformed through the subspace of the healthy structure's PCs, using the same matrix V^T to transform the data back to its original dimension.

$$Y_{transformed} = Y_{reduced} \times V_{reduced}^T \quad (8)$$

However, if the structure has been altered as a result of damage, this transformation will not effectively reconstruct the data. The Root Mean Square Error

(RMSE) is used to measure the discrepancy between the original data matrix and the transformed data. This reconstruction error (damage index) will be high, if the structure has been altered as a result of damage. If the error for a certain measurement is higher than the selected threshold, it is classified as damaged.

2.3.3 Anomaly Detection Autoencoder

An Autoencoder (AE) is used to learn effective codings from unlabeled data, making use of a smaller dimensionality representation of the input. In the encoding phase, the input vector $y \in \mathbb{R}^M$ is given to the algorithm to map it into the code h . In the simplified scenario, where there is one single hidden layer, this process can be written as:

$$h = z^1(W^1 y + b^1)$$

Where W^1 and b^1 are the weights and biases of the encoding layer, respectively, and z^1 denotes the activation function, generally a nonlinearity. Through the decoding stage, the output of the hidden layer h is rebuilt to the original dimensions y' , using the weights and biases of the decoding layer, W^2 and b^2 , as well as the activation function z^2 :

$$y' = z^2(W^2 h + b^2)$$

This algorithm optimizes all weights and biases using the backpropagation process, which aims to minimize the following cost function E (Equation 9).

$$E = \frac{1}{N} \sum_{n=1}^N \sum_{m=1}^M (y_{k,n} - y'_{k,n})^2 \quad (9)$$

During training, the AEs learn how to recover a subset of healthy input data from the encoding. When the AE reconstructs data measured from a damaged blade it is not effective, since the data can not be represented from the same encoding learned. Similarly to the PCA method, a damage index is defined by calculating the RMSE difference between the reconstruction and the input to determine whether the structure is damaged or healthy.

3. Experimental Campaign

The measurements for this study were conducted in two rounds of the experimental campaign. For each round, vibration-based data, including acceleration time-series and FRFs, were collected. On the first stage, data of a blade in its healthy state was collected, for the purpose of model updating. On the following phase, the response of the blade in healthy and damaged states was gathered, to be used at a later stage to develop damage detection algorithms.

In spite of having different purposes, both experimental campaigns were conducted very similarly, so both setups are the same.

The experiments on the scaled Glass-Fiber Reinforced Polymer (GFRP) blade were carried out in clamped-free boundary conditions, the blade was fixed to an aluminium plate. The response of the system was

measured in terms of acceleration making use of of ten accelerometers placed along the back of the blade. Six uniaxial and four triaxial, therefore a total of eighteen measured degrees-of-freedom (DOFs). All the data acquisition was made using the Simcenter Testlab software with the parameters found in Table 1 through a Simcenter SCADAS.

Table 1: Testlab acquisition parameters

Bandwidth [Hz]	800
Spectral lines	2048
Acquisition time [s]	2.56
Estimator	H1

Over the course of this thesis, for both the damage detection techniques and the numerical simulation approach, the accelerometers are named according to the number given to the position where they are placed (Figure 1).

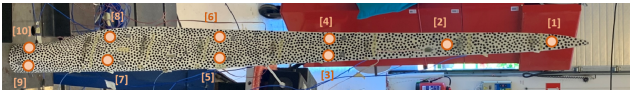


Figure 1: Ten locations of the accelerometers.

3.1. Measurements for Model Updating

The Simcenter 3D finite element model of the blade in question is updated using response data collected from experimentally testing the scaled blade. The data used in this procedure must be very reliable, so an investigation was performed to assess what excitation force better excites this system. The two options in consideration were modal hammer testing and modal shaker testing. In order to choose between the two, first the best material for the tip of the hammer was determined, followed by the appropriate signal for the shaker to send to the blade. After reaching these conclusions, a comparison between the best results from each of the testing options was made, and the method which produced the best results was selected. The quality indicator functions used to compare the results were the coherence, the Power Spectrum Density (PSD) and the Frequency Response Function (FRF).

For the modal hammer the choice was between rubber, metal or plastic tip. After comparing the functions it was concluded that the rubber tip is not able to excite the entire range of interest (800Hz) and that the metal tip does not behave well for lower frequencies. The material selected was the plastic.

When performing modal shaker testing, the choice was between three types of excitation signals: periodic chirp, continuous random and pseudo random. After analysing the indicator functions of each signal, it was visible that the periodic chirp signal provides more energy to the structure and the continuous random signal is noisier. It was concluded that the periodic chirp signal was the strongest choice.

Ultimately, the only decision left was between modal hammer testing with a plastic tip or modal shaker testing with the periodic chirp signal. Looking at the qual-

ity indicator functions it was clear that the impact testing does not excite the structure as accurately as the modal shaker. Furthermore the modal shaker testing is far more practical than the modal hammer testing from an experimental standpoint. So, the best experimental data for model updating resulted from conducting modal shaker tests employing a periodic chirp signal. From this point forward, these are the measurements being analysed.

The vibration data collected by the accelerometers was processed in the Simcenter Testlab software and the model parameters were estimated internally using the Polymax algorithm as explained in Section 2.2. The stabilization diagram obtained from this data is in Figure 2, where the stable poles for the frequency range 8-650Hz are already selected. Subsequently to the stable pole selection, the algorithm's estimated parameters are as indicated in Table 2

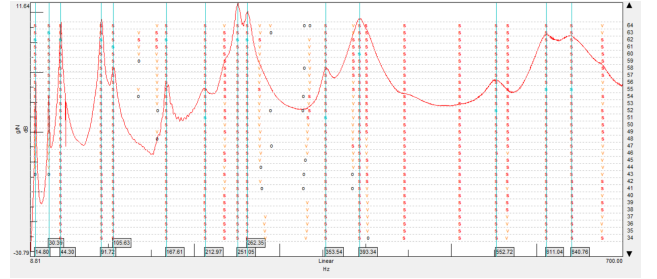


Figure 2: Polymax stabilization diagram.

3.2. Measurements for Damage Detection

Within the scope of damage detection through Machine Learning algorithms, there is a need for vibration response data of the structure in its healthy and damaged state. In order to obtain this experimental data, tests were carried out with the scaled blade. The source of the excitation force was the same modal shaker, however, two different signals were used: continuous random signal and sine excitation signal. With intent to simulate operational conditions of a wind turbine and in the framework of fatigue testing, respectively.



Figure 3: Seven locations of the masses.

The damaged states were simulated by placing seven nuts of different masses, one at a time, in seven different locations of the front of the blade (Figure 3). As shown in Table 3, the smallest damage used represents 0.063% of this mass and the largest one is 1.233%. By varying these masses, the intent is to simulate various damage scenarios and conclude on the sensitivity of the algorithms tested in Section 4.

Table 2: Estimated modal parameters.

Natural Frequency (Hz)	14.80	30.39	44.30	91.72	105.63	167.61	212.97	251.05	262.35	353.54	393.34	552.72	611.04	640.76
Damping Ratio (%)	1.80	1.58	2.51	2.17	2.50	1.99	3.79	1.53	1.59	1.89	2.39	2.27	2.15	2.56

Table 3: Masses of the nuts used.

Mass [g]	Relative mass [%]
0.5	0.063%
0.7	0.088%
1	0.126%
2.1	0.264%
2.8	0.352%
4.7	0.591%
9.8	1.233%

4. Damage Detection

The purpose of this section is to assess damage detection methodologies, so, with the experimentally measured data, a variety of algorithms was tested: Multivariate Gaussian Anomaly Detection (MGAD), Principal Component Analysis (PCA) and Anomaly Detection Autoencoders (ADAE). In agreement to what was explained in Section 3.2, these algorithms make use of data generated from using continuous random and sine signals. In the diagram of Figure 4, the methodologies are summarized.

4.1. Multivariate Gaussian Anomaly Detection

4.1.1 Implementation

The MGAD makes use of the natural frequencies estimated from each measurement to verify the structure’s health. These features are estimated from the FRF data collected during the experimental campaigns. The FRFs are first put through the Polymax algorithm, then an automated modal parameter selection algorithm is used to select the stable poles and estimate the modal parameters (natural frequencies, damping ratios and mode shapes). Finally, using a reference modeset, the estimated modal parameters undergo a modal tracking process, pairing the reference and automatically selected modes.

Therefore, from the automated modal analysis technique the machine learning algorithm receives a dataset containing the vectors of natural frequencies for each experimental run described in Section 3.2. The full dataset described is then divided into three different data subsets. The training stage only makes use of the healthy data, therefore, 70% of the undamaged runs went into the training subset, the remaining were split equally between the validation and the test subsets. The damaged runs were divided evenly between the validation and test subsets.

After the healthy natural frequencies are fitted into a multivariate Gaussian distribution and the probability density function defined, the optimal threshold is selected. Lastly, the test subset is put through the algorithm and the examples are classified as damaged or undamaged.

Since the experimental testing was performed under different circumstances, the complexity of the dataset increases. Because the method used for the feature estimation is automated and not manual, there is difficulty in identifying a few natural frequencies. Consequently, the damage detection algorithm receives a matrix with missing features for some examples. A function was developed that runs through the dataset and identifies the possible combinations of missing features. The algorithm then proceeds to operate normally, but obtaining results separately for each of those instances, overcoming this problem.

4.1.2 Results

On the one hand, the experimental runs of the blade in its healthy state present considerable frequency intervals for some natural frequencies. On the other hand, for lower magnitude damages, specially if placed closer to the root, the results present negligible changes. Both these factors contribute for the difficulty of the natural frequencies representing accurately the state of the structure, which jeopardises the performance of the algorithm.

The issues identified before are reflected on the accuracy of the algorithm, which has a value of 77.9%.

The Receiver Operating Characteristic (ROC) curve illustrates the search for the optimal threshold as a function of the false positive rate (x axis) and the true positive rate (y axis). When looking at the MGAD ROC curve, in Figure 5, there is a rather high false positive rate for the optimal threshold found, which indicates that this algorithm is wrongly classifying a large number of healthy examples as damaged.

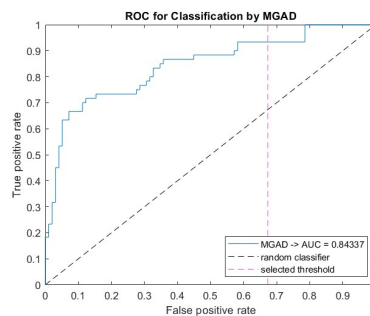


Figure 5: MGAD ROC curve

4.2. Implementation of PCA and ADAE

The PCA and ADAE algorithms use FRFs and time-series generated from using continuous random and sine signals as input. On one hand, PCA was utilized due to its ability to apply linear algebra operations to find a reduced subspace capable of representing the structural health of the blade. While the use of ADAE tests the ability of a nonlinear algorithm with the same

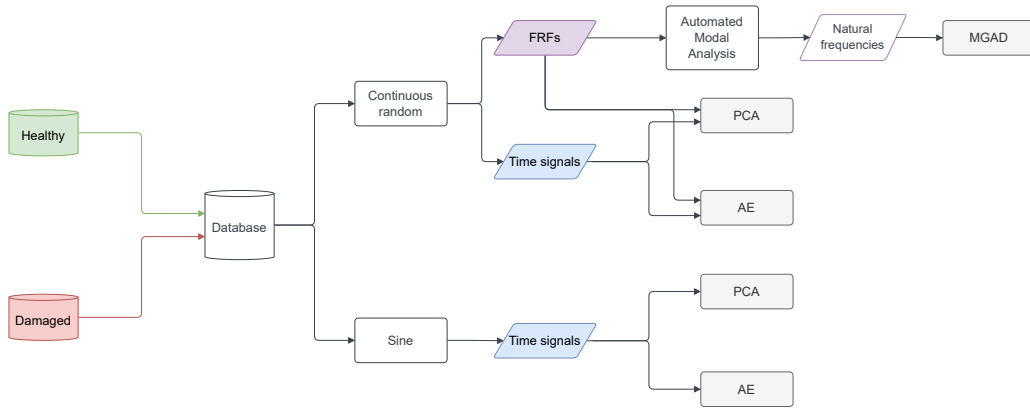


Figure 4: Methodologies developed for damage detection.

objective. The testing dataset is classified based on its reconstruction error (damage index), if the error of a certain point exceeds the established threshold, it is classified as an anomaly. The underlying assumption is that it will be difficult to successfully recover data measured for the blade that contains structural changes like damage.

Analogously to what was described for the implementation of MGAD in Section 4.1, training, validation, and test subsets were extracted from the complete dataset using the same percentages.

4.2.1 Results PCA

When using data measured using the continuous random excitation, the FRFs achieved an accuracy of 93.2% and the time-series an accuracy of 81.4%. Only few FRF measurements were misclassified, mostly damaged runs with the smaller magnitudes of damage and placed closest to the root, which are the hardest damages to detect. The performance of the algorithm on the time signals was considerably lower, having misclassified all healthy measurements as damaged. The PCA algorithm doesn't work as well for the time-series as it does for the FRFs. This makes sense from the standpoint that the FRF vectors are representative of the system, whereas the time-series, each feature is a point in time of response to a random excitation, so these values might have no connection between measurements. Therefore, the reconstruction of the time data is not that effective even from one healthy dataset to another.

The results from the time-series response dataset to a sine excitation reached an accuracy of 70.3%. Once again, all healthy runs were classified as damaged. Similarly to the continuous random time-series dataset, the algorithm can't learn how to represent the structure from the data resulting from a sine excitation. Since this is a signal which only excites one frequency, there is not enough information in the response of the structure that could describe its state.

The Area Under Curve (AUC) is the area under a ROC curve. The AUC is an overall summary of diagnostic accuracy. AUC equals 0.5 when the ROC curve corresponds to random chance and 1.0 for perfect ac-

curacy. As seen in Figure 6 the value obtained from implementing FRF data is very high, approximately 0.99, indicating the usefulness of this method for damage detection. On the other hand, in Figure 7, the AUC of the damage detection technique using time-series data is low, around 0.58, not far from a random chance classifier. The ROC curve from implementing sine excitation data also takes an unfavorable shape (Figure 8). Once again, the time data obtained an AUC result similar to a random classifier, 0.54.

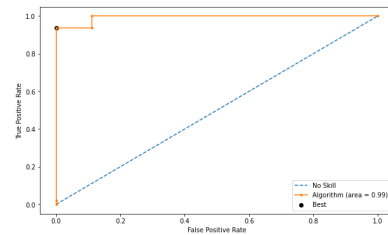


Figure 6: PCA continuous random FRFs ROC curve

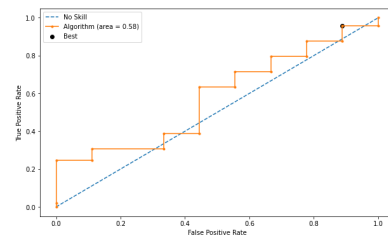


Figure 7: PCA continuous random time-series ROC curve

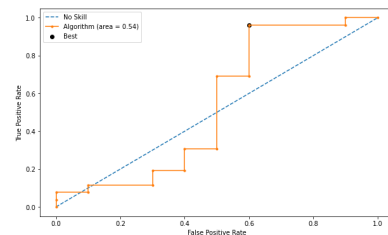


Figure 8: PCA sine time-series ROC curve

4.2.2 Results ADAE

Regarding the responses from a continuous random excitation, the FRF results obtained 93.2% accuracy

and the time-series 83.1% was recorded. The results were extremely similar to the ones observed with the PCA, only a few FRF measurements with less significant damage were overlooked and all time signal data was classified as damaged. An accuracy of 70.3% was reached by the results from the time-series response dataset to a sine excitation, being that all healthy measurements were classified as damaged. The ROC curves for each methodology was identical to the results of the PCA.

Since the outcome was the same as using the PCA algorithm, the ADAE corroborates the fact that this time-series response data is not enough to represent the structure's state. Therefore, it is proven that using this input data is not a good methodology.

5. Computational Simulations

To apply and develop more accurate and complex machine learning approaches for structural health monitoring, simulation data could be used. If the goal is to use these damage detection techniques in real life structures, the simulated data should be as accurate as possible. For this, high fidelity models need to be developed, here is where the search for model updating strategies comes in. There is a need to develop these strategies to validate and update the models in accordance with real data.

In this work, a model updating process was developed, where experimental data measured from the physical GFRP scaled blade is compared to the data generated from simulations with the FE model of the blade. The finite element model of the blade undergoes an updating process. First, introducing the appropriate clamped boundary conditions, with the FE model of the blade the vibration response was generated in the time (SOL 112) and frequency (SOL 111) domain modal response solvers from Simcenter 3D. These results were compared with the experimental measurement results (Section 3.1) and the simulation model was updated accordingly.

5.1. Simulation Baseline Model

The finite element model of the GFRP wind turbine blade was produced by DTU, using their in-house Blade Modelling Tool [11].

5.1.1 Modal Frequency Response Analysis

The modal frequency response analysis (SOL 111) computes the structural response to an oscillatory excitation explicitly defined in the frequency domain. An excitation force applied on the node corresponding to coordinates of the shaker cell, was added to the undamped structure by importing a *.csv* file of the force magnitude in the frequency domain. This file results from applying the Fourier transform function to the signal used experimentally, measured with the sensors in the cell of the shaker. The response of the blade was requested to the SOL 111 in the form of acceleration per forcing frequency, in the range 8 to 700Hz. The output result's format was a *PUNCH* file, containing the requested acceleration information, for each node

with corresponding coordinates with an accelerometer position. In postprocessing, a MATLAB® script was developed that read this file and saved the acceleration information for each of the 18 DOFs.

After reading the predicted acceleration data, the Frequency Response Functions were computed. Figure 9, shows the plot of the simulation FRF, for accelerometer 3 measuring in the out-of-plane direction, juxtaposed with the same FRF obtained experimentally. The red curve has a very different shape from the reference FRF, the experimental peaks are lower and get wider throughout the range, while the simulation resonances are higher in amplitude and narrower. This is clearly characteristic of the contrast between a damped and an undamped system. Therefore, to generate reliable simulation data, the damping effect needs to be taken into account. The process of introducing this information and the resulting FRFs are presented in the upcoming Section 5.2.

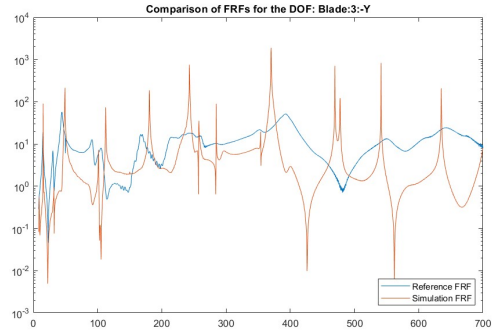


Figure 9: Baseline simulation FRF (in red) vs. experimental FRF (in blue).

5.1.2 Modal Transient Response Analysis

Conducting a similar procedure for the time domain simulations, the modal transient response analysis (SOL 112) was performed. The excitation force was applied in the same node, still to the undamped structure. However, the excitation force was defined in the time domain, for each time-step instead of forcing frequency.

The acceleration was plotted as a function of time. In Figure 10, a comparison is made between the response in the time domain of the reference structure (in blue) and the finite element simulation (in red). The two signals are strikingly different. While the resonance effects are clear in the experimental curve, the simulation response is less transparent. This might result from the fact that the simulation model does not account for damping, once again, the damping effects are proven to be needed for an accurate representation of this composite structure's response. The technique used for the addition of this information to the FE model is explained in the following section 5.2.

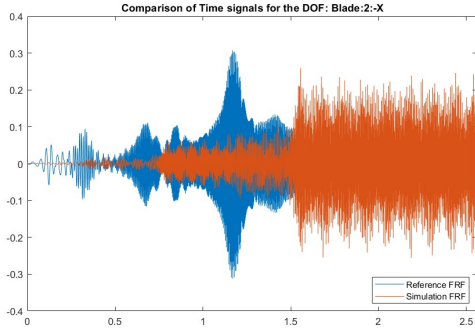


Figure 10: Baseline simulation acceleration time signal (in red) vs. experimental time signal (in blue).

5.2. Introducing Damping

The modal response solvers have a unique functionality, where modal damping values can be introduced and applied to each mode independently. In this study, this tool was taken advantage of, by making use of the modal damping ratios estimated from the experimental data measured. The values in Table 2 are introduced in the model.

5.2.1 Modal Frequency Response Analysis

The excitation force, in the frequency domain, was applied to the damped model of the blade and its acceleration response was saved for each DOF. Then, each FRF was computed. Figure 11, shows the new simulation FRF plot for the DOF being analyzed and its experimental reference curve. The improvement of the correlation between the two, when compared with the undamped results in Figure 9, is evident.

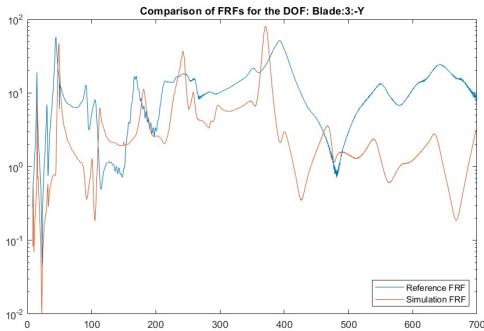


Figure 11: Damped model simulation FRF (in red) vs. experimental FRF (in blue).

5.2.2 Modal Transient Response Analysis

In the time domain analysis, the damped system response was calculated for the same input force scenario described previously. The response as acceleration time signals for each DOF was compared with the one obtained experimentally and showed a much more similar curve, as seen in Figure 12. The resonance peaks are now visible, happening approximately on the same points in time and with similar amplitudes at first.

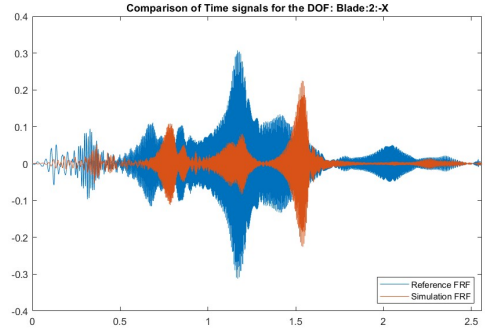


Figure 12: Damped model simulation acceleration time signal (in red) vs. experimental time signal (in blue).

5.3. Model Optimization

For the model updating process the software used was Simcenter HEEDS. Considering that two different types of data are being used to compare the measured and the FE model's predicted responses - the FRFs and the time-series -, two independent studies were implemented. One with the goal of minimizing the difference between the FRFs and another that attempted to minimize the difference between the time domain acceleration response data. For both these studies, 18 variables were defined, these were each of the materials Young's modulus and mass density. The shell of the blade being studied is made of fiberglass epoxy composite materials (UD, BIAx, UNIAX), closer to the root, aluminium is used for the clamping to the rotor and the shear web of balsa wood is bonded to the shell with glue.

The responses to the optimization process were metrics defined to evaluate the correlation between the experimental and simulation datasets. The similarity metric used for the FRF data was the Frequency Response Assurance Criterion (FRAC), which assesses the correlation between the pairs of FRF vectors (Equation 10).

$$FRAC = \frac{\|\hat{y} \cdot y^T\|^2}{\|\hat{y}\|^2 \|y\|^2} \quad (10)$$

When comparing the simulation acceleration time signals with the ones obtained experimentally an error metric was used (Equation 11), the Root Mean Square Error (RMSE). For either study, the objective defined was to minimize the corresponding difference between responses.

$$RMSE = \sqrt{\frac{\sum_{i=1}^N \|y(i) - \hat{y}(i)\|^2}{N}} \quad (11)$$

To process the data and calculate these metrics two MATLAB scripts were developed. To each HEEDS project, the Simcenter 3D blade model was added as the input file along with the MATLAB script as the output file. Making use of a tool called 'Analysis Portals', HEEDS is able to access the values of the defined variables in the model as well as the responses computed in the scripts. Since these files are connected within HEEDS, the search for the optimal design begins. An iterative process is conducted, where, as the

values of the material properties are changing, the resulting correlation metrics are extracted. The study is complete when the number of designs tested corresponds to defined number of evaluations desired. This iteration process is schematized in the diagram of Figure 13.

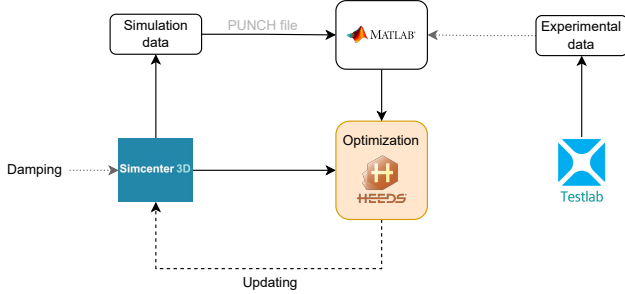


Figure 13: Model updating workflow between the three software.

5.3.1 Modal Frequency Response Analysis

For the optimization study in the frequency domain, using SOL 111, after searching for the best design, the material properties that minimized the FRAC difference were returned by HEEDS. With the new set of material properties applied on the model, SOL 111 simulation was ran and new set of FRFs was numerically generated. An optimized FRF can be seen in Figure 14 as the red curve.

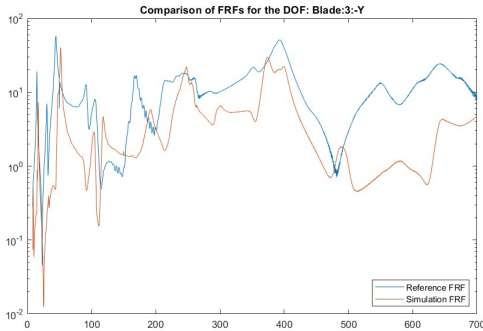
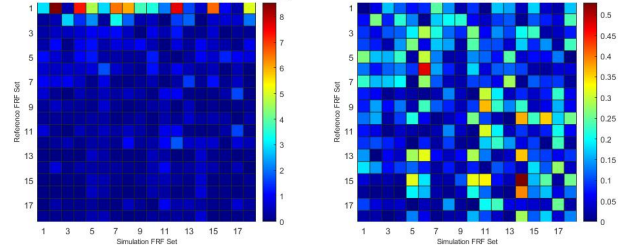


Figure 14: Updated model simulation FRF (in red) vs. experimental FRF (in blue).

A more detailed assessment can be made of the FRF data using the FRAC matrix. This metric correlates the FRF vectors measured for each DOF, so the matrix can illustrate the improvements. Figure 15 shows the initial FRAC matrix correlating the reference FRFs with the vectors generated with the initial undamped baseline model (a) and with the FRFs predicted by the updated model (b).

The optimized FRAC matrix shows significant improvement from the baseline. The initial matrix shows no correlation between the FRFs, while, the optimized has a few diagonal entries that appear to have found correlation. Quantifying these changes resorting to the RMSE, there was an overall improvement of 70.51% in correlation.



(a) Baseline. (b) Optimized.

Figure 15: FRAC matrix.

5.3.2 Modal Transient Response Analysis

After conducting the optimization in the time domain (SOL 112), HEEDS returned the design which minimized the RMSE between the time signals.

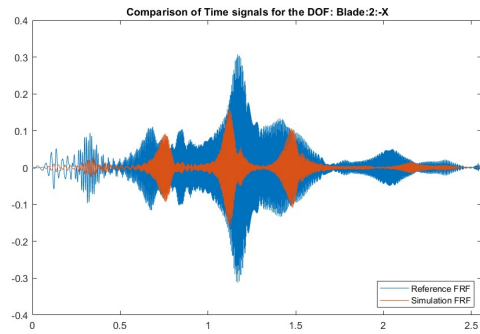


Figure 16: Updated model simulation acceleration time signal (in red) vs. experimental acceleration time signal (in blue).

The evolution of the RMSE between the time-series measured experimentally and generated by the FE model is quantified as a 31.00% improvement, from the baseline to the optimized model. This is noticeable when Figures 10, 12 and 16 are compared.

6. Conclusions

In this thesis, through experimental procedures on a scaled GFRP wind turbine blade, a data base was developed using three different excitation signals (continuous random, sine and periodic chirp). These robust response data enabled the implementation of different methodologies for both damage detection and model updating.

Three different anomaly detection algorithms were tested, each with a distinct approach. The MGAD, centred on the premise that a shift in natural frequencies is indicative of damage. This premise was confirmed, for multiple damage scenarios, although it failed for some of the analyzed small scale damage scenarios. The natural frequencies proved not to be sensible enough for the detection of these minor damages, while also being subject to other parameters which influenced these features and were not accounted for (i.e. boundary conditions, temperature). The PCA and ADAE algorithms are based on the abnormal reconstruction error of damaged data (damage index). For this, a subspace of representation of healthy data was learned and then used to reconstruct data back to

its original dimension. This methodology was implemented using a linear algebra formulation by PCA and using non-linear neural network encodings by ADAE. The features used by both techniques were the vibration responses on two domains: time and frequency. The FRF vectors were proven to be representative features, showing clear variation for most damaged structures. The response time signals, from continuous random and sine excitation, however, were not representative features of the structure's state. The use of time-series proved not to be a good methodology, so other features might need to be extracted from this data, in order for the algorithms to achieve success.

The FE model and simulation methodologies were guided towards a reliable representation of the dynamic behaviour of the real blade, using the physical structure's response to a periodic chirp excitation signal. The simulation vibration results were obtained for the time (SOL 112) and frequency (SOL 111) domains, considering the response of the FE model of the blade with respect to an experimental excitation. The initial simulated results had a big discrepancy when compared to the measured experimental data, mainly from the FE model disregarding damping behavior by default. So modal damping estimated by Polymax from the experimental data was input into the model. This step turned out to be crucial for obtaining meaningful simulation data. These results were further improved by optimizing FRFs and time-series data using the optimization software HEEDS. The material properties of the FE model were updated, so that the simulation matched the experimental data, with correlation improvements up to 70% from the baseline.

6.1. Future Work

The methodologies developed in this thesis have a long way to go before they can be implemented reliably. A few steps can be taken to advance the applicability of the suggested methods to operational conditions.

In damage detection, new features can be explored, testing the same or new algorithms. Tackling the operational context, instead of using FRFs, the Cross Power Spectral Densities could be calculated. Furthermore, other data sources may be relevant for analysis including surface velocity from a laser Doppler vibrometer and displacements from digital image correlation. More complex algorithms could be tested, in order to explore and analyze data not only from an anomaly detection point of view, but also for assessing and localizing damage.

In respect to model updating, different model variables could be tuned, for example the boundary conditions. This could be done by performing the optimization, while defining the stiffness of the boundary condition as a variable. Different metrics can be defined for the correlation of the data (Modal FRF Assurance Criterion, Time Response Assurance Criterion). The response of the FE model could also be generated while simulating damage.

Ultimately, the future goal would be to combine the two fields studied in this thesis. After gathering reliable

simulation data from an updated FE model, apply it to the damage detection algorithms as training examples.

Acknowledgements

The author would like to thank Eng. André Guilherme Massano Tavares and Prof. Nuno Miguel Rosa Pereira Silvestre for all the support given.

References

- [1] B. Jorgensen, H. Holttinen, IEA wind TCP annual report 2020, Tech. rep., IEA Wind Technology Collaboration Programme (August 2021).
- [2] M. Martinez-Luengo, A. Kolios, L. Wang, Structural health monitoring of offshore wind turbines: A review through the statistical pattern recognition paradigm, *Renewable and Sustainable Energy Reviews* 64 (2016) 91–105. doi:10.1016/j.rser.2016.05.085.
- [3] C. R. Farrar, K. Worden, *Structural Health Monitoring: A Machine Learning Perspective*, John Wiley Sons, LTD, 2013. doi:10.1002/9781118443118.
- [4] Y. Wang, M. Liang, J. Xiang, Damage detection method for wind turbine blades based on dynamics analysis and mode shape difference curvature information, *Mechanical Systems and Signal Processing* 48 (1-2) (10 2014). doi:10.1016/j.ymssp.2014.03.006.
- [5] Siemens Product Lifecycle Management Software Inc., NX Nastran, *Basic Dynamic Analysis User's Guide* (2014).
- [6] Siemens Support Center, What is operating modal analysis?, <https://community.sw.siemens.com/s/article/OMG-What-is-OMA-Operating-Modal-Analysis>, last accessed on 03-08-2022.
- [7] W. Heylen, S. Lammens, P. Sas, *Modal Analysis Theory and Testing*, 2nd Edition, Katholieke Universiteit Leuven, Faculty of Engineering, Department of Mechanical Engineering, Division of Production Engineering, Machine Design and Automation, Leuven, 2007.
- [8] D. J. Ewins, *Modal Testing, Theory, Practice and Application*, John Wiley Sons, Inc., 1984.
- [9] B. Peeters, H. V. D. Auweraer, P. Guillaume, J. Leuridan, The polymax frequency-domain method: A new standard for modal parameter estimation?, *Shock and Vibration* 11 (3-4) (01 2004). doi:10.1155/2004/523692.
- [10] P. Guillaume, P. Verboven, S. Vanlanduit, H. V. D. Auweraer, B. Peeters, A poly-reference implementation of the least-squares complex frequency-domain estimator, *Proceedings of IMAC 21* (1 2003).
- [11] M. Peeters, G. Santo, J. Degroote, W. V. Paepegem, High-fidelity finite element models of composite wind turbine blades with shell and solid elements, *Composite Structures* 200 (05 2018). doi:10.1016/j.compstruct.2018.05.091.